Matching different symmetries with an atomically sharp interface: Epitaxial Ba_2SiO_4 on Si(001)

Julian Koch,[1,*] Knut Müller-Caspary,[2] and Herbert Pfnür[1,3,†]

[1] *Institut für Festkörperphysik, Leibniz Universität Hannover, Appelstraße 2, 30167 Hannover, Germany*
[2] *Ernst Ruska-Centre for Microscopy and Spectroscopy with Electrons, Forschungszentrum Jülich, 52425 Jülich, Germany*
[3] *Laboratory of Nano and Quantum Engineering (LNQE), Leibniz Universität Hannover, Schneiderberg 39, 30167 Hannover, Germany*

(Dated: November 10, 2019)

In this study we present a comprehensive investigation of the epitaxial growth of Ba_2SiO_4 on Si(001), a system in which neither crystal symmetry nor lattice constants match in a simple manner. In addition, it has the potential to become the first crystalline high-k gate dielectric. We combined X-ray photoelectron spectroscopy (XPS), low energy electron diffraction (LEED) and aberration-corrected scanning transmission electron microscopy (STEM) in order to optimize the epitaxial growth by molecular beam epitaxy. Our focus was on the formation of a high quality crystalline interface. The films were grown by a co-deposition method that requires no diffusion of Si from the substrate. 400 °C turned out to be sufficient to form chemically homogeneous films. However, crystalline films require an annealing step to $670-690$ °C for the formation of the epitaxial interface necessary for breaking Si-O bonds. STEM confirms that the interface is atomically sharp and that a single layer of the silicate is changed to a (2×3) structure at the interface from the (2×1.5) bulk structure. Based on our experimental results, we propose a geometrical model for the epitaxial interface. The growth of films with an under-stoichiometric Si flux leads to the formation of a near surface Ba silicide that does not restrict the epitaxial silicate growth.

I. INTRODUCTION

Ultrathin oxide films in combination with semiconductors can be viewed as prototype systems on which formation of interfaces, conditions of growth and defect densities have been studied in detail [1–3]. They are of ever-increasing scientific and technological interest, since they provide many possibilities of functionalization and application, such as the use as a gate insulator for field effect transistors [4], wave guides [5], barriers for tunnel junctions and spin filters [6]. The interfaces of these materials can exhibit properties that are completely different from those of the corresponding bulk. For example, ferromagnetism or superconductivity can emerge at interfaces of materials that are non-magnetic or non-conducting, respectively, in the bulk [6, 7].

The interface between silicon surfaces and dielectric layers is of particular technological interest for the continued scaling of CMOS transistors. In order to achieve the best possible scaling using a planar transistor structure, the formation of an atomically sharp interface with an extremely low defect concentration, surpassing even the SiO_2/Si interface, is required. The most promising pathway in this direction is the growth of crystalline gate oxides [8–10]. McKee et al. have demonstrated that epitaxial $BaTiO_3$ can be grown with very small trapped interface charge density ($D_{it} < 10^{10}$ eV^{-1}cm^{-2}) using a layer sequencing technique to manipulate the interface [11]. Nonetheless, a crystalline gate oxide that fulfills all of the requirements placed upon high-k gate dielectrics [4] is still missing to date. In the case of $BaTiO_3$, the band gap is too small for practical application. Epitaxial $Ba_{0.7}Sr_{0.3}O$ layers, lattice matched to Si(001), are thermodynamically not sufficiently stable in contact with silicon and turn into silicate at temperatures above 400 °C [12].

Epitaxial Ba_2SiO_4 on Si(001) is a candidate that could potentially fulfill all requirements for a crystalline gate oxide. Interestingly, this material was shown to grow as crystalline layers on Si(001) [13, 14], although neither symmetry (tetragonal vs. cubic) nor lattice constants match in a simple manner between the two systems. Ba_2SiO_4 grows with its longest crystal axis perpendicular to the Si(001) surface. The lattice constants in the other two crystal directions are approximately equivalent to 2 and 1.5 times the Si lattice constant in [1 1 0] direction, respectively (lattice constants of orthorhombic Ba_2SiO_4: $a = 7.51$ Å$, b = 5.81$ Å$, c = 10.21$ Å [15], S(001): $a = 3.84$ Å).

Furthermore, Barium silicates are thermodynamically and kinetically very stable. In particular, the reaction of the oxides SiO_2 and BaO to silicate is exothermic [16]. Generally, silicates are spontaneously generated from the oxides, as shown in several examples in the past [13, 17–19], and these silicate layers are stable up to their desorption temperature above 750 °C. The thermal stability is thus comparable to SiO_2. Moreover, Ba_2SiO_4 also fulfills other requirements necessary for high-k materials. Epitaxial films have shown a dielectric constant of 22.8 ± 0.2, band offsets to p-Si(001) of over 2 eV and an acceptable leakage current of 3 mA/cm^2 at -1 V [14]. The only problem is that these films still featured a high density

* koch@fkp.uni-hannover.de
† pfnuer@fkp.uni-hannover.de

of interface traps of $D_{it} = (1 \pm 0,5) \times 10^{13}\,\mathrm{eV}^{-1}\mathrm{cm}^{-2}$. This interface property is closely related to the formation of the film itself, for which diffusion of Si from the Si(001) substrate into a deposited BaO layer was used, which leads to an atomically rough interface, only works in presence of concentration gradients of Si, and thus may introduce local disorder and/or local variations of composition.

In order to avoid the diffusion problem, we used a co-deposition growth method in the present study, in which Ba and Si were evaporated simultaneously in an oxygen atmosphere. In the following, we show that a precise control of the oxygen background pressure and the individual fluxes is a prerequisite for high quality Ba_2SiO_4 thin films with an atomically sharp interface. Furthermore, we analyze the formation and structure of the epitaxial interface in order to understand how the lattice matching is achieved and develop an appropriate model.

II. EXPERIMENTAL METHODS

Ba_2SiO_4 layers with thicknesses between 1 and 16 nm (4 and 63 monolayers (ML)) were prepared under UHV conditions (base pressure $8 \cdot 10^{-11}$ torr) on Si(001) samples (size $6 \times 14\,\mathrm{mm}^2$, p-type, B doped, resistivity 10 to 20 $\Omega\,$cm) by molecular beam epitaxy.

The Si samples were cleaned ex situ with purified water ($\rho > 18\,\mathrm{M}\Omega\,\mathrm{cm}$), petroleum ether, acetone and isopropanol in an ultrasonic bath for 15 min per step. Then they were dipped in HF solution (1 %) until the oxide was completely removed (i.e. for approximately 30 s), as indicated by a hydrophobic surface, followed by a controlled reoxidation in H_2O_2 solution (35 %, 40 s). After each step, the samples were rinsed in purified water. In vacuum, the samples were degassed for more than 12 hours at temperatures up to 600 °C and subsequently trained by heating to temperatures between 700 and 800 °C for a few minutes per step. Finally, the oxide film was removed by flash annealing to 1050 °C.

Ba_2SiO_4 films were grown by evaporation of Ba from a crucible and of Si from a rod, both heated by electron bombardment, in an oxygen background pressure. Fluxes were controlled by a quartz crystal microbalance at sample position, which was also used to calibrate relative thicknesses. The films were grown at room temperature in order to minimize oxidation of the Si surface and Si diffusion from the substrate. At the beginning of the growth, 0.5 ML Ba were first deposited before the Si flux was added. Subsequently, oxygen was introduced into the chamber and the oxygen partial pressure was carefully increased to its final value within 30 s after the addition of the Si flux. The deposition rate was 1.1 ML/min. The films were annealed using direct current heating at temperatures between 400 and 700 °C for 30 to 40 min. The temperatures were determined with a pyrometer (min. 300 °C) with emission coefficients adjusted to Si. In particular, $\varepsilon = 0.574$ was used for T = 680 °C. The optimum annealing temperature and oxygen background pressure will be discussed below. Annealing was always carried out in vacuum without oxygen. A new Si sample was used for each film.

The BaO film was grown similar to the Ba_2SiO_4 films but without the Si flux. The SiO_2 film was gown by thermal oxidation and its thickness was measured by ellipsometry.

The Ba_2SiO_4 films were investigated using a high resolution low energy electron diffraction system (SPA-LEED), X-ray photoelectron spectroscopy (XPS) and aberration-corrected scanning transmission electron microscopy (STEM). The SPA-LEED and XPS investigations were performed in situ. The XPS spectra were recorded with a SPECS Phoibos 100 spectrometer with an MCD-5 detector using an Al K_α source. The energy scale of the XPS system was calibrated using the Si 2p peak of a clean Si substrate (99.15 eV binding energy). For the evaluation of the XPS data a Shirley background was first subtracted and the O 1s peaks were then fitted with an LA(1.5,1.5,100) type peak in CasaXPS [20]. This line shape is a convolution of a Lorentzian and a Gaussian, and with the given parameters symmetric. It was carefully chosen since it perfectly describes the O 1s peaks of 16 nm thick BaO and Ba_2SiO_4 films, both of which feature single O 1s peaks.

In order to compare integrated XPS intensities the measuring conditions have to be identical for both measurements, i.e. the instrument has to be in the exact same state and the sample has to be in the exact same position. We ensured the first part by keeping the instrument running when the measurements were performed on the same day, i.e. when comparing the same sample before and after annealing. When the measurements were performed on different days (Fig. 2a)), the instrument was turned off between the measurements, however, all potentiometers were locked in place and only on/off-switches were used so that the applied voltages and currents remained the same for all measurements. Also, only measurements from one measurement period were compared, with no bake-out of the system in between. Furthermore, the manipulator is equipped with micrometer screws that allow the sample to be reliably put in the same position for every measurement. The identical measuring conditions were ultimately confirmed by the background levels being the same for the compared measurements.

For the ex situ STEM investigations the samples were capped with 1 ML of Si followed by 300 nm of Au. Two cross-sectional TEM lamellae in $[1\,1\,0]$ and $[1\,\bar{1}\,0]$ Si zone axes have been prepared using a focused ion beam (FIB) facility with a final low-energy milling step in order to remove amorphised surface layers arising from previous milling steps. The two zone axes were used to obtain structural images of the epitaxial layer in two projections rotated by 90°. Scanning Transmission Electron Microscopy was performed using a FEI Titan 80/300 STEM instrument equipped with an aberration corrector for the probe-forming lens [21]. The microscope was operated at 200 kV, and high-angle annular dark field

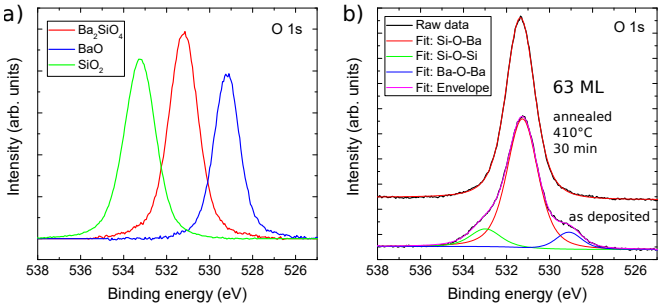

Figure 1. Identification of chemical bond formation from the chemical shift of the O 1s signal in XPS: a) Amorphous layers of BaO (blue line, 16 nm thick), SiO_2 (green, 18 nm) and Ba_2SiO_4 (red, 16 nm, annealed at 400 °C) on Si(001) are compared. The intensity of the SiO_2 peak was not calibrated with respect to the others. b) O 1s signal of a 16 nm (63 ML) thick Ba_2SiO_4 film, as deposited at room temperature (bottom curve) and after annealing at 410 °C (top curve). The deconvolution into the individual components is shown by colored lines as indicated in the inset.

(HAADF) Z-contrast STEM images were acquired using a Fischione 3000 detector at a camera length of 135 mm. The final absolute thickness calibration of the Ba_2SiO_4 films was done using these STEM images.

III. RESULTS AND DISCUSSION

A. Stoichiometry and chemical homogeneity

The exact ratio between the Si and Ba fluxes was carefully adjusted for stoichiometric growth conditions since this ratio turned out to be non-self-limiting. The oxygen concentration, on the other hand, is self-limiting *in the bulk* as long as the oxygen partial pressure is high enough for a complete oxidation of the films. Under this condition, the oxygen content of the films is only determined by the Si and Ba fluxes, as confirmed from the O1 s signal in XPS: Neglecting interface contributions, this XPS signal does not change at fixed Ba and Si fluxes even if the oxygen pressure is increased by one order of magnitude. As it turned out, the line shape of the O 1s peak in XPS is ideal to identify any deviation from the Ba_2SiO_4 stoichiometry, and thus to calibrate the system. The relative chemical shift between the covalent bonds in SiO_2, and the ionic bonds in BaO is approximately 4 eV for O 1s, as demonstrated in Fig. 1a), where we compare the O 1s signals of BaO and SiO_2 with that of Ba_2SiO_4. All films are at least 16 nm thick, so that the interface contribution to the signals is negligible. Conveniently, every O atom in the particular silicate compound we are interested in, Ba_2SiO_4, is bound to exactly one Si atom, i.e. no Si-O-Si bonding states are present [22], in contrast to other barium silicate compounds like $BaSiO_3$ [23] or $BaSi_2O_5$ [24]. This results in a single O 1s peak for Ba_2SiO_4, which is located roughly in the middle of the SiO_2 and BaO peaks, as also shown in the figure. This chemical oxidation state will be referred to as Si-O-Ba bonding state in the following. The energy difference of about 2 eV between the peaks can easily be resolved by a standard XPS. Therefore excess concentrations of Si or Ba lead to clearly visible shoulders at higher or lower binding energies, respectively. It is important to see these peaks as a representation of chemical bonding states and not of compounds, since a shoulder at higher binding energy, in particular, can be either due to local SiO_2 or to a barium silicate compound with a higher Si concentration than Ba_2SiO_4.

We first adjusted the Si and Ba fluxes to the required ratio of 1:2, using a quartz crystal microbalance located at sample position, by weighting the changes in frequency over time with the atomic masses. In order to confirm that we have obtained the correct Si:Ba atomic ratio in the deposited films, a 63 ML (16 nm) thick Ba_2SiO_4 film was grown. Since the contribution of the interface to the XPS signal is negligible at this thickness, the peak shape is only determined by the Si to Ba ratio. The O 1s peaks after deposition at room temperature (RT) and after annealing at 410 °C for 30 min are shown in Fig. 1b). Directly after deposition the O 1s peak has two shoulders with approximately the same area. This demonstrates that the reaction at RT is incomplete so that local deviations from stoichiometry lead to various bonding characters and to only about 80% preference for the Si-O-Ba bonding state. Only after annealing to 410 °C, which does not lead to any desorption, a single peak at the Si-O-Ba position is formed, i.e. the reaction is complete. As expected, this peak has approximately the same integrated intensity as the RT peak including the shoulders. This symmetric peak demonstrates that the correct deposition ratio for stoichiometric deposition was chosen. Furthermore, it shows that temperatures around 400 °C are sufficient for getting a *chemically* homogeneous film. This temperature, however, is too low to crystallize amorphous layers. In fact, all films starting with an amorphous interface layer turned out to remain amorphous after an annealing step to 400 °C.

B. Interface properties and oxygen pressure

In contrast to the bulk material, the interface between the silicate and the Si(001) surface is highly sensitive to the background oxygen pressure. On the one hand, this is due to the oxidation of the Si(001) surface, which leads to the formation of amorphous SiO_x. On the other hand, the Si wafer acts as a reservoir for Si so that the formation of Si-rich silicate compounds is possible, irrespective of the Si flux. Both effects limit the crystalline quality of the deposited film. In order to achieve high quality epitaxial films with an abrupt interface, it is therefore absolutely essential to fine tune the oxygen partial pressure to a value just above the saturation point for complete oxidation.

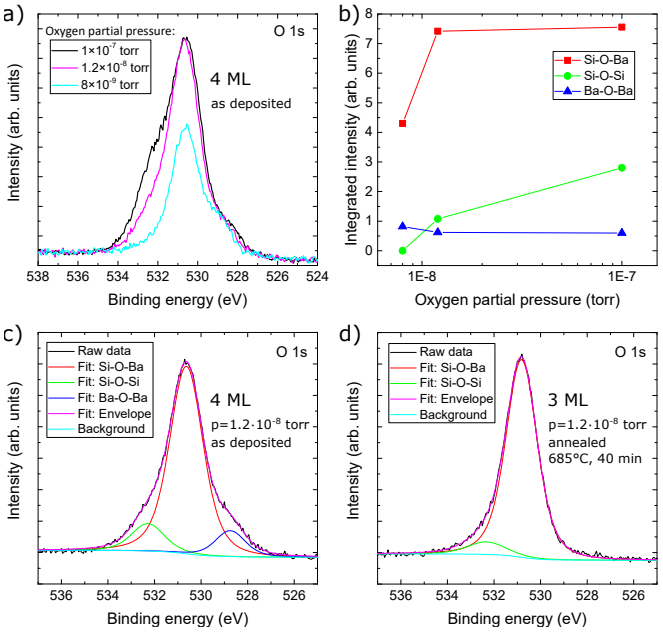

Figure 2. Determination of the optimal oxygen background pressure: a) XPS O 1s spectra for (approximately) 4 ML thick Ba-silicate layers grown with different oxygen background pressures. The spectra were taken directly after growth at room temperature. The Si/Ba ratio was kept at the optimal value as determined in the context with Fig. 1. b) Integrated intensities of contributions from different chemical bonding environments obtained from fits of the curves in a). An example of this fit is shown in c) for the optimal oxygen partial pressure of $1.2 \cdot 10^{-8}$ torr. d) O 1s peak after annealing the layer in c) to 685°C for 40 min.

For calibration of the oxygen partial pressure, we again use the line shape of the O 1s peak in XPS, but this time we investigate ultrathin films so that the interface is visible. For this purpose, we grew 4 ML thick films at a rate of 1.1 ML/min in different oxygen partial pressures using the stoichiometric Si:Ba ratio determined above. The corresponding O 1s peaks and the integrated intensities of their individual components are shown in Figs. 2a) and b), respectively. Since the spectra were taken directly after growth at RT, the reaction is still incomplete and thus all peaks feature a component at the BaO position. Nevertheless, the conclusion is still clear: 1.2×10^{-8} torr is the optimum oxygen partial pressure for this growth rate. For positive deviations from this optimum pressure the concentration of O atoms in Si-O-Si bonding states is increased significantly, while the concentration of O atoms in Si-O-Ba bonding states stays nearly constant, indicating an oxidation of the silicon surface. At negative deviations the main peak at the Si-O-Ba position is drastically reduced, indicating an oxygen deficiency for silicate formation.

The O 1s peaks for a 4 ML film grown at optimum conditions before and after annealing at 685 °C for 40 min are shown in Figs. 2c) and d), respectively, together with the deconvolution into the individual components. During the annealing process, about 1 ML of the film was desorbed, as derived from the intensity of the Ba 3d and O 1s peaks in XPS, so that the 4 ML film was reduced to only 3 ML after annealing. Even after annealing, the O 1s peak of the now 3 ML thick film still shows a small concentration of O atoms in Si-O-Si bonding states, unlike the peak of the 63 ML film. This concentration remains unchanged when the film is grown with a small Ba excess. Therefore, this signal is most likely due to interface bonds that are required between the film and the substrate, and is not due to defects. Assuming that the O atoms in Si-O-Si bonding states sit in the monolayer closest to the interface and that this layer has the same oxygen concentration as the overlying layers, the Si-O-Si signal corresponds to a concentration of 1/4 ML. In order to correct for the damping of the signal by the overlying layers we used an inelastic mean free path of 2.072 nm calculated with the TPP-2M equation using the NIST Electron Inelastic-Mean-Free-Path Database [25].

The important difference to all previous steps, however, is the appearance of a crystalline film after annealing. When using stoichiometric Ba and Si fluxes, crystallinity was only achieved when the oxygen background pressure during growth was close to the saturation point. While lower oxygen pressures will not allow to obtain stoichiometric conditions, higher pressures lead to oxidation of the interface (see Fig. 2b)) that prevents crystalline growth.

This behavior is in strong contrast to conditions of large Ba excess concentrations. Islam et al. [14] obtained crystalline Ba_2SiO_4 thin films by Si diffusion from the substrate into a BaO film (BaO contains twice as much Ba per O atom as Ba_2SiO_4) even though the oxygen background pressure during the growth of the BaO film was one order of magnitude above the saturation point determined in this work at a comparable growth rate, i.e. a SiO_x must have formed at the interface.

If Si is supplied by diffusion from the substrate, it is the ratio of Ba:O in the system that determines the silicate formation, which is always thermodynamically favorable to keeping either SiO_2 or BaO in the system [16]. Under conditions of large Ba excess Ba_2SiO_4 is formed predominantly, since it is the Ba-silicate compound with the highest Ba concentration. Therefore, as long as there is sufficient excess Ba in the system, a SiO_x layer at the interface does not prevent the formation of crystalline Ba_2SiO_4, since it can be incorporated into the Ba_2SiO_4 film during reactive growth, thus scavenging interfacial SiO_x in favor of silicate formation. However, when we start with a stoichiometric Ba_2SiO_4 layer, and force the system to incorporate additional SiO_x at the interface, the formation of silicate compounds with higher Si concentrations than Ba_2SiO_4 will occur for thermodynamic reasons [16]. These compounds again hinder the epitaxial growth of Ba_2SiO_4 due to their crystal structures that do not match to Si(001). We tested this hypothesis by growing films with a *reduced* Si flux, i.e. a BaO surplus. In-

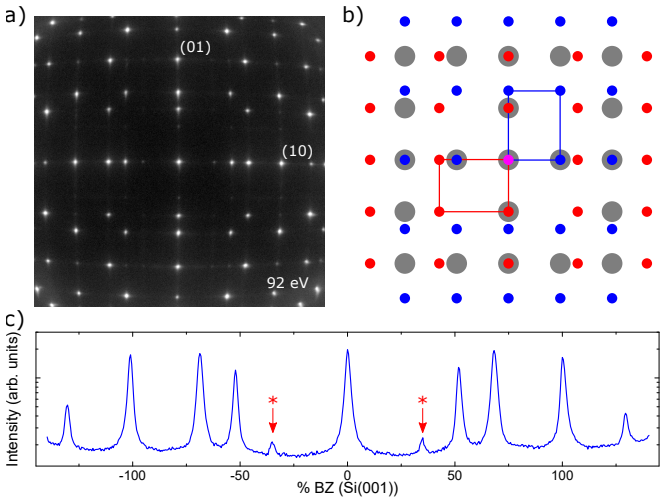

Figure 3. LEED pattern of epitaxial Ba_2SiO_4: a) LEED image of a 3ML film after annealing to 685 °C taken at 92 eV. The film was grown under optimal conditions as determined from Figs. 1 and 2. b) Schematic of this pattern with two orthogonal rectangular unit cells (red and blue dots), demonstrating epitaxial growth with axes a, b of the silicate $\parallel$ Si[1$\bar{1}$0]. Gray balls indicate the positions of the diffraction spots of the Si(001) substrate prior to silicate deposition. c) Horizontal line scan through the center of a). Spots marked by $*$ are not indicated in b).

deed, when the Si flux was reduced by 50%, crystallinity could still be achieved even with an oxygen partial pressure 50 times higher than the saturation pressure from above.

C. Formation of the epitaxial interface

As mentioned, the key to the growth of high quality crystalline films under stoichiometric Ba:Si ratios is the correct adjustment of the oxygen partial pressure. However, an annealing step at high temperatures close to desorption is still required to crystallize the films. The minimum temperature at which crystallinity was achieved is 640 °C, but the quality was still rather poor and most films even remained amorphous at this temperature. An annealing temperature of $670-690$ °C produced the best and, most importantly, reproducible results. At these temperatures there was already a slight evaporation of the film, as mentioned above, which drastically increased at temperatures above 690 °C. This reduction in thickness was most evident for very thin films, while for more than 40 ML thick films the material loss during annealing was negligible.

The LEED image of the same 3 ML film whose O 1s peak is shown in Fig. 2d) is presented in Fig. 3a). The LEED pattern originates from the superposition of two rectangular domains rotated by 90°. Their reciprocal lattice constants are very close to one half and two thirds, respectively, of the reciprocal lattice constant of the unreconstructed Si(001) surface. Thus, they correspond to the two shorter real space lattice constants a and b of the Ba_2SiO_4 crystal structure, while the c-axis is oriented normal to the surface ($a = 7.51$ Å, $b = 5.81$ Å, $c = 10.21$ Å [15]). A schematic of this structure in reciprocal space is shown in Fig. 3b). The same structure was found in Ref. 14.

As seen from the line profile in horizontal direction through the center of Fig. 3a), shown in Fig. 3c), there are some less intense spots, which correspond to a (2×3) structure. These can be explained by a modulation with twice the lattice constant in the b-direction close to the interface (see below). Since the value of $2b$ is close to three times the silicon lattice constant, it is conceivable that the epitaxial growth leads to a doubling of the lattice constant in this direction close to the interface.

The high-angle annular dark field (HAADF) z-contrast STEM images in Fig. 4 confirm that the interface between the crystalline Ba_2SiO_4, grown under the optimized conditions, and Si(001) is atomically sharp. Whereas the HAADF-STEM technique clearly shows Ba in the epitaxial layer, the Si and O atoms are not visible within the silicate layer due to their low atomic number compared to Ba. Projections along Si[110] are shown. As expected from Fig. 3, two orientations of Ba_2SiO_4 can be seen in this projection, which are depicted in Fig. 4a) and b). As can be seen there, the bulk crystal structure of Ba_2SiO_4 is maintained up to the penultimate layer at the interface, i.e. only one layer at the interface is geometrically modified, neglecting relaxations, in order to form the bonds to the Si(001) substrate. The Ba atoms that are shifted from their bulk positions in Ba_2SiO_4 are depicted in dark green in the overlaid crystal structures. This rearrangement of the Ba atoms at the interface results in a period doubling at the interface in b-direction as compared to the Ba_2SiO_4 bulk structure in this layer, as visible in Fig. 4a). Furthermore, there are only three Ba atoms instead of four within this period. This confirms that the (2×3) structure observed in LEED (see Fig. 3) is indeed due to the epitaxial interface. In the perpendicular direction (see Fig. 4b)) the size of the unit cell at the interface is the same as in the bulk, again in agreement with the LEED data, but clear shifts of Ba atoms at the interface can be seen.

Based on the information from XPS, LEED and STEM and the chemical boundary conditions that Ba atoms are divalent and that the Ba-O bonds are ionic, we have designed a plausible model of the interface, which is depicted in Fig. 5. The model has six O atoms per unit cell in Si-O-Ba bonding states in the interface layer. The (2×1) reconstruction of the Si(001) surface is for the most part still present (see Fig. 5b)). The model only deviates from the Si(001) (2×1) reconstruction at two Si atoms per interface unit cell. Here the bonds are elongated by an O bridge. Thus these Si atoms can get closer to the Ba atom in the second silicate layer so that ionic bonds can be formed. The concentration of O atoms in Si-O-Si

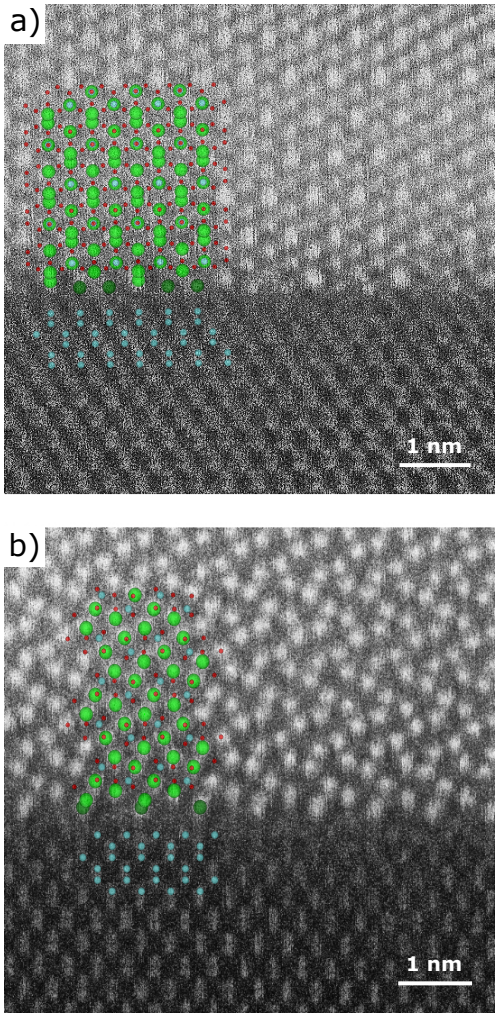

Figure 4. High-angle annular dark field (HAADF) z-contrast STEM images: a) b, c-projection and b) a, c-projection of the Ba_2SiO_4 crystal structure. The bright spots are Ba atoms. The bottom of both images shows the Si(110) plane. The images were taken from a 44 ML Ba_2SiO_4 film, which was prepared by first growing a crystalline 3 ML film under optimized conditions. Then an additional 41 ML were deposited at RT and the film was annealed at 680 °C for 40 min. The crystal structures overlaid on the images were drawn with VESTA [26] based on Refs. 22 and 27. Green: Ba, blue: Si, red: O. The Ba atoms at the interface that deviate from the Ba_2SiO_4 bulk structure are depicted in dark green.

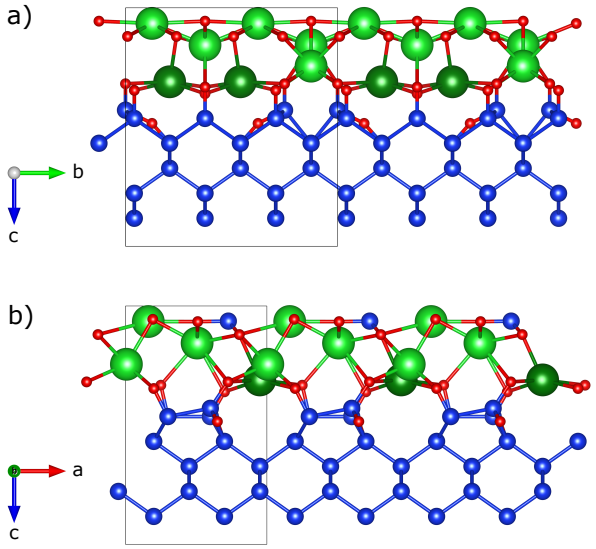

Figure 5. Proposed interface model: a) b, c-projection and b) a, c-projection with respect to the Ba_2SiO_4 crystal structure. Green: Ba, blue: Si, red: O. The structure was drawn with VESTA [26]. In this model, the Ba_2SiO_4 bulk structure [22] was slightly streched so that the a and b axes fit exacly 1:2 and 2:3, respectively, to the lattice constant in [1 1 0] direction of the Si lattice [27], i.e. small lattice mismatches were ignored. The Ba atoms at the interface that deviate from the Ba_2SiO_4 bulk structure are depicted in dark green.

bonding states, two per interface unit cell, is equivalent to 1/4 ML of the Ba_2SiO_4 bulk structure and thus in agreement with the XPS results shown in Fig. 2d). The pseudo (2×1) reconstruction results in a 1:1 match in a-direction between Ba_2SiO_4 and the Si surface.

We now deal with the question why the high temperature annealing step is necessary for the formation of crystalline layers. Even though no long range diffusion is necessary to form the silicate, since conditions very close to the perfect stoichiometry were chosen, the formation of crystalline layers still requires the same high temperature step as under conditions of silicate formation by Si diffusion [14]. It is clear from the LEED images that the crystallization has to start at the interface, since the film is perfectly aligned with the substrate and there is no rotational disorder. Moreover, when we deposited an additional 4 ML on a crystalline 3 ML film, the film could already be crystallized by annealing to 400 °C. The crystalline quality was comparable to that of the initial film. We tested this method up to a thickness of 63 ML and always obtained crystalline layers at 400 °C, though with slightly decreasing crystal quality for the thickest films as evident from the spot profile in LEED, which could be improved after annealing to higher temperature. Hence, the high annealing temperature is only needed to form the epitaxial interface.

An adjustment of the stoichiometry at the interface cannot be the reason for the requirement of the high temperature, since Si is already sufficiently mobile at lower temperatures. As an example, we investigated the reaction of a 1 nm thick BaO film with Si by diffusion from the Si bulk. Annealing at 400 °C for 30 min was sufficient to turn this film completely into silicate.

The high temperature is also not needed to break the original (2×1) reconstruction of the Si(001) surface, since it is possible to produce crystalline films with an oxygen partial pressure during growth that is more than one order of magnitude above the saturation point, if

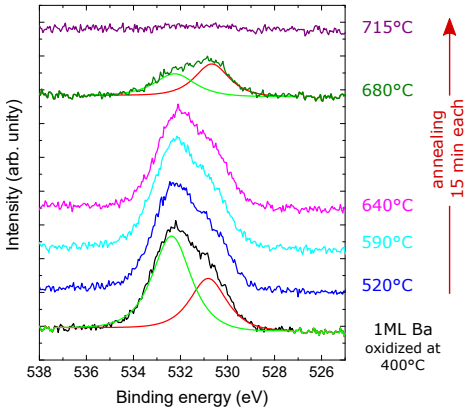

Figure 6. Effects of high temperature annealing on the interface: A 1 nm thick Ba film on Si(001) was oxidized in an oxygen partial pressure of $5 \cdot 10^{-8}$ torr for 10 min at 400 °C and subsequently annealed at increasing temperatures for 15 min per step. The O 1s spectra after oxidation and after each annealing step are shown. For the spectra after oxidation and after annealing to 680 °C the deconvolution into the individual components (Si-O-Si green, Si-O-Ba red) is also shown. The spectra were shifted for better visibility.

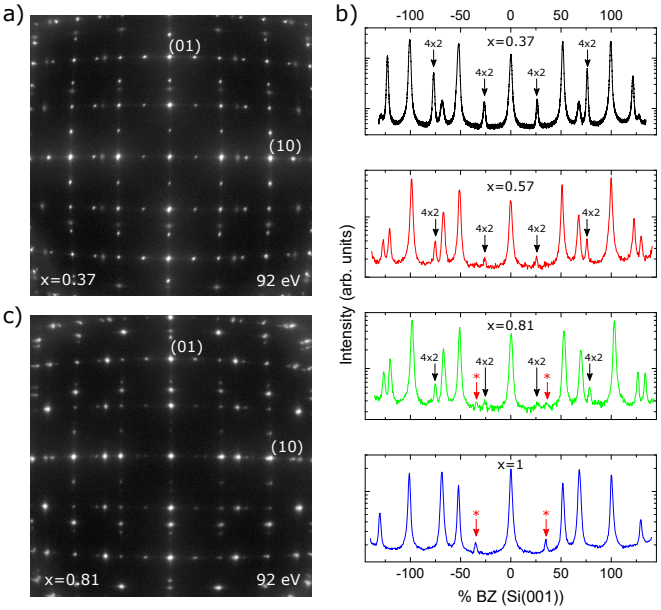

Figure 7. Effects of an under-stoichiometric Si flux on the interface: 4 ML films were grown with a reduced Si flux and subsequently annealed to 685 °C. x denotes the normalized Si flux, with $x = 1$ corresponding to the flux needed for the exact stoichiometry of Ba_2SiO_4. The LEED images for $x = 0.37$ and 0.81 are shown in a) and c), respectively. The horizontal line scans through the center of the LEED patterns for $x = 0.37$, 0.57, 0.81 and 1 are shown in b).

the additional oxygen concentration at the interface is compensated by lowering the Si flux and thereby indirectly lowering the oxygen content of the bulk (see section III B). In this case the (2×1) reconstruction at the interface is definitely destroyed, due to the oxidation of the Si(001) surface. However, the high temperature step is still needed to crystallize these films.

In order to better understand the effect of the high temperature annealing step on the interface we deposited one monolayer of Ba on a Si(001) surface and oxidized it at 400 °C. Then we annealed it at increasing temperatures for 15 min per step. The corresponding O 1s peaks are shown in Fig. 6. Directly after oxidation at 400 °C the O 1s peak consists of two components at the Si-O-Si and Si-O-Ba locations with a ratio of roughly 2:1. The annealing steps at 520 °C and 590 °C have no effect on the peak. At 640 °C the Si-O-Si component is already slightly reduced. At 680 °C the Si-O-Si component is reduced significantly, whereas the Si-O-Ba component is only slightly reduced. Finally, at 715 °C the oxygen is completely desorbed.

The temperature range at which the Si-O-Si peak is reduced lines up perfectly with the temperatures needed for crystallization of the Ba_2SiO_4 films. In particular, the temperature at which the reduction of the Si-O-Si peak sets in, is exactly the lowest temperature at which crystallization was observed. These findings indicate that the high temperatures required for the formation of the epitaxial interface are needed to break interfacial Si-O bonds for O atoms with two bonds to Si, possibly for O atoms with two bonds to the substrate. Under our conditions the transient formation of this type of bonds could not be avoided, not even by starting with an amorphous monolayer of Ba.

If we assume the proposed interface model in Fig. 5 to be correct, the high temperature can be explained by the need to (largely) restore the (2×1) reconstruction of the Si(001) surface that was destroyed by oxidation during the silicate growth, and by the need to reduce the concentration of Si-O-Si to 1/4 th of a monolayer.

D. Robustness of crystalline growth: Ba excess concentrations

Finally, we tested the robustness of the interface when modifying the composition of ultrathin layers and its consequence on crystalline silicate growth. 4 ML films (given as the necessary Ba amount) were grown, again at RT, with a reduced Si flux of $x = 0.37$, 0.57, 0.81 and 1 times the flux needed for the exact stoichiometry of Ba_2SiO_4. As expected, the O 1s peaks of the Si deficient layers (not shown here) show a larger BaO fraction than the stoichiometric film that increases with decreasing x. After annealing at 685°C for 40 min all films turned completely into silicate due to Si diffusion from the substrate. While the thickness of all films was reduced during the annealing, the reduction in thickness increased with increasing Si deficiency. A possible reason is the lower initial amount of O atoms per Ba atom and desorption of

Ba during annealing (there was no oxygen background pressure during annealing). The thicknesses of the films after annealing were 1.6, 2.3, 2.5 and 3 ML for $x = 0.37$, 0.57, 0.81 and 1, respectively, as derived from the Ba 3d and O 1s peaks in XPS.

The LEED images for $x = 0.37$ and 0.81 as well as the line scans through the (00) and (10) spots after annealing for all films are shown in Fig. 7. As expected from the discussion in section III B, the varying concentrations of Si relative to Ba do not suppress the formation of crystalline silicate layers. The interesting part, however, is the appearance of a faint, but quite sharp (4×2) structure for $x < 1$ that we assign to the formation of a near-surface Ba silicide, following Ref. [28]. The high intensity of the (4×2)-peaks for $x = 0.37$ is most likely due to the smaller film thickness. The absence of the (4×2) structure for $x = 1$, however, seems to be real, since the presence of the (2×3) structure (spots marked with $*$) associated with the epitaxial interface means that the interface is still visible in LEED at this thickness. Moreover, neither a (4×2) structure nor Ba diffusion into the substrate was observed in STEM, see Fig. 4. Therefore, the appearance of the (4×2) structure seems to be coupled with a surplus of Ba or BaO in the insulator film. While most of the Ba seems to desorb during the annealing process, there is also the possibility of diffusion of Ba to the Si interface and the subsequent formation of silicide [28–30].

Crystalline silicate formation turns out to be quite robust with respect to these variations of the interface. While a sharp (2×1.5) structure appears under all conditions in LEED, the disappearance of the (2×3) structure for $x = 0.57$ and 0.37 indicates that the silicide distorts the period doubling. This does not necessarily mean that the local structure is changed. Only long range order is distorted.

IV. CONCLUSIONS

We have demonstrated that epitaxial Ba_2SiO_4 thin films can be grown on Si(001) with an atomically sharp interface and investigated the formation of this interface. In order to match Ba_2SiO_4 with its (2×1.5) structure to Si(001) a (2×3) structure is needed at the interface. However, the system is flexible enough so that this change in crystal structure from the Ba_2SiO_4 bulk structure is limited to only one layer at the interface. Considering the Ba_2SiO_4 crystal structure, the cause for this flexibility are most likely the undirected Ba-O bonds that hold the SiO_4 tetrahedra together. The formation of the epitaxial interface neither requires a special surface preparation nor intentional lattice matching. Only well optimized growth conditions are needed. The stability of this system is further demonstrated by the fact that the crystalline growth is not prevented by silicide formation at the interface.

The key to the successful growth of crystalline films in this study was the precise determination of the saturation point for the oxygen background pressure based on the line shape of the O 1s peak in XPS. This method might also be helpful for the growth of other oxide species on silicon, since it is, according to our experience, more precise than methods based on the frequency change of a quartz crystal microbalance.

As mentioned in the introduction, Ba_2SiO_4 has many attractive properties for a high-k dielectric, and may serve as a crystalline high-k gate insulator. For this purpose, the precise definition of the epitaxial interface is a necessary and important step. Furthermore, the proposed interface model can serve as a starting point for theoretical investigations. This work may also provide a basis for controlled manipulation of the epitaxial interface.

Acknowledgement K.M.-C. acknowledges funding from the Initiative and Network Fund of the Helmholtz Association under Contract No. NG-1317.

[1] E. J. Tarsa, K. L. Mccormick, and J. S. Speck, Common Themes in ther [sic] Epitaxial Growth of Oxides on Semiconductors, MRS Proceedings **341**, 73 (1994).

[2] J. Lettieri, J. H. Haeni, and D. G. Schlom, Critical issues in the heteroepitaxial growth of alkaline-earth oxides on silicon, Journal of Vacuum Science & Technology A: Vacuum, Surfaces, and Films **20**, 1332 (2002).

[3] Y. Segal, J. W. Reiner, A. M. Kolpak, Z. Zhang, S. Ismail-Beigi, C. H. Ahn, and F. J. Walker, Atomic Structure of the Epitaxial BaO/Si(001) Interface, Physical Review Letters **102**, 116101 (2009).

[4] J. Robertson and R. M. Wallace, High-K materials and metal gates for CMOS applications, Materials Science and Engineering: R: Reports **88**, 1 (2015).

[5] Z. Liu, P.-T. Lin, B. W. Wessels, F. Yi, and S.-T. Ho, Nonlinear photonic crystal waveguide structures based on barium titanate thin films and their optical properties, Applied Physics Letters **90**, 201104 (2007).

[6] M. Bibes, J. E. Villegas, and A. Barthélémy, Ultrathin oxide films and interfaces for electronics and spintronics, Advances in Physics **60**, 5 (2011).

[7] A. D. Caviglia, S. Gariglio, N. Reyren, D. Jaccard, T. Schneider, M. Gabay, S. Thiel, G. Hammerl, J. Mannhart, and J.-M. Triscone, Electric field control of the $LaAlO_3/SrTiO_3$ interface ground state, Nature **456**, 624 (2008).

[8] R. A. McKee, F. J. Walker, and M. F. Chisholm, Crystalline Oxides on Silicon: The First Five Monolayers,

Physical Review Letters **81**, 3014 (1998).
[9] M. B. Nardelli, F. J. Walker, and R. A. McKee, Crystalline oxides on semiconductors: a future for the nanotransistor, physica status solidi (b) **241**, 2279 (2004).
[10] C. J. Först, C. R. Ashman, K. Schwarz, and P. E. Blöchl, The interface between silicon and a high-k oxide, Nature **427**, 53 (2004).
[11] R. A. McKee, Physical Structure and Inversion Charge at a Semiconductor Interface with a Crystalline Oxide, Science **293**, 468 (2001).
[12] D. Müller-Sajak, S. Islam, H. Pfnür, and K. R. Hofmann, Temperature stability of ultra-thin mixed BaSr-oxide layers and their transformation, Nanotechnology **23**, 305202 (2012).
[13] D. P. Norton, C. Park, Y. E. Lee, and J. D. Budai, Strontium silicide termination and silicate epitaxy on (001) Si, Journal of Vacuum Science & Technology B: Microelectronics and Nanometer Structures **20**, 257 (2002).
[14] S. Islam, K. R. Hofmann, A. Feldhoff, and H. Pfnür, Structural, Dielectric, and Interface Properties of Crystalline Barium Silicate Films on Si(100): A Robust High-κ Material, Physical Review Applied **5**, 054006 (2016).
[15] G. Pieper, W. Eysel, and T. Hahn, Solid Solubility and Polymorphism in the System Sr_2SiO_4-Sr_2GeO_4-Ba_2GeO_4-Ba_2SiO_4, Journal of the American Ceramic Society **55**, 619 (1972).
[16] R. Barany, E. G. King, and S. S. Todd, Heats of Formation of Crystalline Silicates of Strontium and Barium, Journal of the American Chemical Society **79**, 3639 (1957).
[17] M. El Kazzi, G. Delhaye, C. Merckling, E. Bergignat, Y. Robach, G. Grenet, and G. Hollinger, Epitaxial growth of SrO on Si(001): Chemical and thermal stability, Journal of Vacuum Science & Technology A: Vacuum, Surfaces, and Films **25**, 1505 (2007).
[18] T. Genevès, B. Domenichini, L. Imhoff, V. Potin, O. Heintz, P. M. Peterlé, and S. Bourgeois, Elaboration and characterization of barium silicate thin films, Micron **39**, 1145 (2008).
[19] T. Genevès, B. Domenichini, L. Imhoff, V. Potin, Z. Li, and S. Bourgeois, Photoemission study of the reactivity of barium towards SiO_x thermal films, Surface Science **605**, 1704 (2011).
[20] Casa Software Ltd, CasaXPS Manual 2.3.15 (2009).
[21] A. Kovács, R. Schierholz, and K. Tillmann, FEI Titan G2 80-200 CREWLEY, Journal of large-scale research facilities JLSRF **2**, A43 (2016).
[22] K. Persson, Materials Data on Ba_2SiO_4 (SG:62) by Materials Project, ID: mp-17612 (2014).
[23] K. Persson, Materials Data on $BaSiO_3$ (SG:19) by Materials Project, ID: mp-7339 (2014).
[24] K. Persson, Materials Data on $BaSi_2O_5$ (SG:62) by Materials Project, ID: mp-3031 (2014).
[25] C. J. Powell and A. Jablonski, NIST Electron Inelastic-Mean-Free-Path Database, Version 1.2, SRD 71, National Institute of Standrds and Technology, Gaitherberg, MD (2010).
[26] K. Momma and F. Izumi, VESTA 3 for three-dimensional visualization of crystal, volumetric and morphology data, Journal of Applied Crystallography **44**, 1272 (2011).
[27] K. Persson, Materials Data on Si (SG:227) by Materials Project, mp-149 (2014).
[28] W. C. Fan and A. Ignatiev, Identification of ordered atomic structures of Ba on the Si(100) surface, Surface Science **253**, 297 (1991).
[29] X. Hu, C. A. Peterson, D. Sarid, Z. Yu, J. Wang, D. S. Marshall, R. Droopad, J. A. Hallmark, and W. J. Ooms, Phases of Ba adsorption on Si(100)-(2×1) studied by LEED and AES, Surface Science **426**, 69 (1999).
[30] K. Ojima, M. Yoshimura, and K. Ueda, Observation of the Si(100)"1×2"-Ba surface by scanning tunneling microscopy, Physical Review B **65**, 075408 (2002).